

The Foundation and Study of the Lattice Inversion Potential for Platinum

REN Xianli¹, CHEN Song^{1*}, LI Longfei², WU Xiangyue¹, BI Yanan¹, XIE Ming¹, WANG Saibei¹

(1. State Key Laboratory of Advanced Technologies for Comprehensive Utilization of Platinum Metal,

Kunming Institute of Precious Metals, Kunming 650106, China;

2. School of Materials Science and Technology, University of Science and Technology Beijing, Beijing 100083, China;)

Abstract: The lattice cohesive curve of Platinum was investigated through first-principles calculations. The double-exponential function to fit the curve was presented. The inversion pair potential curve was generated through Chen's inversion method. The accurate pair potential function was obtained through fitting by the new double-exponential function. The phonon spectra were calculated through using the inversion potential data, the EAM (embedded atom method) potential theory and first principle method respectively to verify the reliability of the inversion potential. The method combining Boltzmann statistics equation with accuracy fitting of lattice cohesive energy curve was proposed to calculate the thermal expansion coefficient. In addition, the bulk modulus and Grüneisen constant in the room temperature were calculated. The results were in good agreement with experiment results, which implied that the inversion potential was effective and accurate.

Key words: Platinum; Lattice inversion; First-principles; Accurate inversion potential

CLC number: TG146.3⁺4 **Document code:** A **Article ID:** 1004-0676(2019)S1-0024-07

铂的反演势的构建与研究

任县利¹, 陈 松^{1*}, 李龙飞², 吴先月¹, 毕亚男¹, 谢 明¹, 王塞北¹

(1. 昆明贵金属研究所 稀贵金属综合利用新技术国家重点实验室, 昆明 650106;

2. 北京科技大学 材料科学与工程学院, 北京 100083)

摘 要: 通过第一性原理计算得到了铂的晶格内聚曲线, 而后利用陈式晶格反演方法, 得到了反演势曲线。利用提出的双指数函数, 拟合得到了精确的铂原子的反演势函数。利用反演势数据、EAM(嵌入式原子法)势理论和第一原理分别计算声子谱, 验证了反演势的可靠性。提出了将玻尔兹曼统计方程与晶格粘聚能曲线精确拟合相结合的热膨胀系数计算方法。此外, 还计算了室温下的体积模量和格鲁内森常数。结果与实验结果吻合较好, 说明计算得到的铂的反演势是有效的、准确的。

关键词: 铂; 晶格反演; 第一性原理; 精确反演势

The potential is the basis of the simulation calculation of condensed matter at atomic scale. The potential function, as foundation of molecular

dynamics method, directly determines the accuracy and reliability of the simulation calculation consequence. Chen's lattice inversion method has

收稿日期: 2019-08-29

基金项目: 国家自然科学基金(51267007, 51461023, U1602275, U1602271)、云南省技术创新人才项目(2016HB024)、云南省自然科学基金(2010CD126, 2012FB195, 2015FA042)

第一作者: 任县利, 男, 博士研究生, 研究方向: 计算材料学。E-mail: renxianli_1@163.com

*通讯作者: 陈 松, 男, 博士, 研究员, 研究方向: 计算材料学。E-mail: cs@ipm.com.cn

been in common use to achieve the pair potentials based on the first-principles calculations, including the fields about rare earth transition intermetallic compounds, metal-ceramic interfaces, ionic crystals and semiconductors^[1-10]. Chen's lattice inversion theory is based on the Möbius transformation in number theory, through strict mathematical proof without any experiential factors. It can obtain the interaction between the central atom and the nearest atom, so that the exact interatomic potential can be obtained. Empirical many-body potential models include adjustable parameters which should be determined by fitting to the experimental data of the involved systems, for example, the EAM potential. Considering the experimental data should be obtained in different physical conditions, the general applicability of empirical many-body potential is not good^[9-11].

In this paper, using the first principles method and Chen's lattice inversion theory^[8-10], the accurate curve of inversion potential of Platinum is constructed. The phonon spectra are calculated through using the inversion potential data. The thermal expansion coefficient of Platinum is calculated, which can provide reference for the study of Platinum.

1 Computational details

1.1 The construction of inversion lattice potential

Based on the Chen's inversion theory^[8-12], the lattice cohesive curve of Platinum is investigated, and the double-exponential function^[8-10] to fit the curve is presented. This can be summed up as a conversion between the following two functions,

$$E(x) = \frac{1}{2} \sum_{n=1}^{\infty} r(n) \varphi(b(n)x) \quad (1)$$

where $E(x)$ is the cohesive energy of atom, x is the nearest atom distance, $r(n)$ is the coordination number of the n th nearest atom, and $b(n)$ is the relative distance of the n th nearest atom.

And then the pair potential between different atoms is written as

$$\varphi(x) = 2 \sum_{n=1}^{\infty} I(n) E(b(n)x) \quad (2)$$

where is inversion coefficient, and can be written as

$$\sum_{b(n)b(m)} I(n) r \left(b^{-1} \left[\frac{b(m)}{b(n)} \right] \right) = \delta_{m1} \quad (3)$$

Assemblage $\{b(m)\}$ satisfying multiplicative semi-group. Using computer programming makes $b(1), b(2), \dots, b(n)$ =from small to large in, and makes $b(1)=1$, $b^{-1}[b(m)/b(n)]$, which is a mathematical operation, has indicate that the value is k by the operation when the value of $b(m)/b(n)$ belongs to the assemblage $\{b(m)\}$ and equal to $b(k)$. Based on the local-density approximation (LDA), the isolated atomic of Platinum ground state energy is obtained through using CASTEP in the Material Studio. The Brillouin-zone is sampled by a $16 \times 16 \times 16$ k -point mesh. The cutoff energy is set to 340 eV. The SCF tolerance is set as 1×10^{-5} eV/atom. The spin polarization is not considered^[13-15]. The calculated ground state energy curve is shown in Fig. 1. The curve is fitted by the following function,

$$\varphi(r) = E_0 + D \exp[-(r - R_0)/\varepsilon] \quad (4)$$

Where E_0 is the ground state energy of isolated atom and $E_0^{\text{Pt}} = -713.60752$ eV.

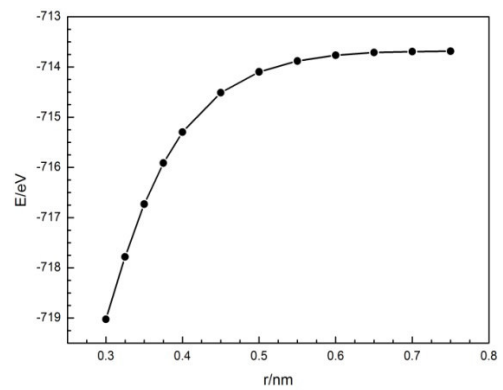


Fig.1 The isolated atomic ground state

图 1 铂单原子能和最近原子距离之间的关系

The lattice cohesive energy in different atomic distances are calculated with distance ranging from 0.2 nm to 1.2 nm, the step length from 0.01 nm to 0.05 nm and a total of 40 grid points. The curve, as shown in Fig.2, is achieved after the value of single atom cohesive energy subtracting the isolated atom ground state energy.

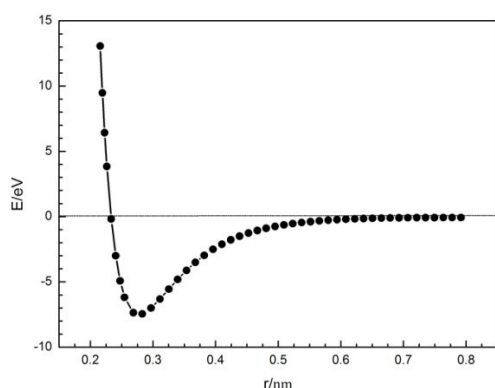


Fig.2 The lattice cohesive energy curve of Pt

图 2 铂的晶格内聚能曲线

According to the above calculation results, the lattice inversion potential curve, which atomic distance from 0.2 nm to 1.2 nm, step length is 0.01 nm and a total of 100 grid points, is obtained by using a self-compiled calculation program, as shown in Fig.3.

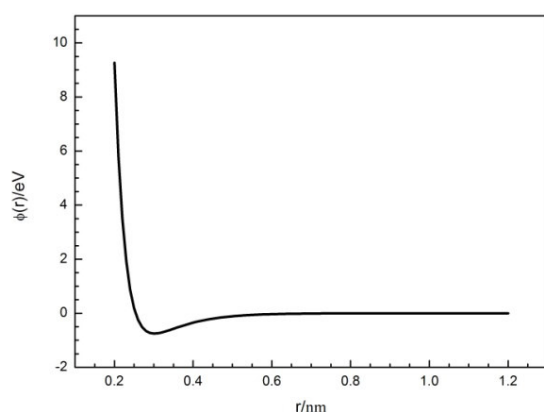


Fig.3 The lattice inversion potential curve of Pt

图 3 铂的晶格反演势曲线

1.2 The fitting of inversion potential function

The exact fitting function, especially the overall consistent function, is the basis for the next precise calculation. The curve shown in Fig.3 is fitted by Origin software, and the quality of the fitting is evaluated by the correlation coefficient given by the software. The correlation coefficient change from 0 to 1, if the value is close to 1, meant that the fitting performance is excellent and the fitting function is accurate. Different potential functions, such as Rose function, Morse function and the new double-exponential potential function proposed in the work are used to fit the lattice inversion potential, and to

compare and analyze the fitting results.

1.2.1 The fitting of Rose function and Morse function

The Rose function is used to fitting the pair potentials^[16], the form is:

$$\phi(r) = -D[1 + \alpha(r - R_0)]\exp[-\alpha(r - R_0)] \quad (5)$$

Where D , R_0 and α represent parameters generated from fitting processing, $\phi(r)$ represents the inversion potential energy, r represents the distance between atoms. The obtained correlation coefficient is 0.99879. The fitting curve matches the points chain very well in the short distance.

Morse function has been in common use to achieve the pair potentials of fcc metal, the form is

$$\phi(r) = D[\exp(-2\alpha(r - R_0)) - 2\exp(-\alpha(r - R_0))] \quad (6)$$

The parameters are listed in Tab.1.

Tab.1 Fitting parameters in Morse potential function

表 1 拟合得到的摩尔斯势参数

| Element | D/eV | $\alpha/(1/\text{nm})$ | R_0/nm |
|---------|---------------|------------------------|-----------------|
| Pt | 0.79636 | 0.153226 | 0.29747 |

The value of correlation coefficient is 0.99911. Comparing the calculation results with the existing data by Flahive P G^[17] is meaningful. The parameters of Morse function is given in Table 2.

Tab.2 Parameters of Morse potential

表 2 摩尔斯势参数

| Element | D/eV | $\alpha/(1/\text{nm})$ | R_0/nm |
|---------|---------------|------------------------|-----------------|
| Pt | 0.7102 | 0.16047 | 0.2897 |

The value of R_0 and α are basically accorded, while the value of D has larger difference. The main reason is the temperature chosen by Table 1 is 0 K, while Table 2 is calculated under gas state. The value of R_0 is determined by the nearest atom distance at equilibrium state, and the value of α is determined by the second derivative of potential function. Although lattice constant will change with the action of atomic vibrations as temperature rose, the equilibrium position remains unchanged. Therefore, both of them are unrelated to the temperature chosen by the potential function. The value of D is relevant to the temperature which relates the difference of minimum

value of inversion potential. Moreover, the base state energy is less than the isolated atomic ground state energy at 0 K under the gas condition. Therefore, the value of D has deviation, and Tab.2 corresponds to smaller value. So the calculated results are precisely accurate.

1.2.2 The fitting of double-exponential potential function equation

The double-exponential potential function is proposed in this work to improve the accuracy in the fitting. The equation containing five parameters is written as

$$\varphi(r) = D_1 \exp[-\alpha(r - R_0)] - D_2 \exp[-\beta(r - R_0)] \quad (7)$$

The value of correlation coefficient is 1, indicating that the fitting quality is excellent. These parameters are listed in Tab.3.

Tab.3 Fitting parameters in double exponential potential function

表 3 双指数函数的拟合参数值

| Element | D_1/eV | $\alpha/(1/\text{nm})$ | D_2/eV | $\beta/(1/\text{nm})$ | R_0/nm |
|---------|-----------------|------------------------|-----------------|-----------------------|-----------------|
| Pt | -1.36137 | 0.114834 | -0.67185 | 0.352749 | 0.283581 |

In order to compare and analyze the effect of three functions fitting on the pair potential curve, the fitting results are zoomed in and analyzed, as shown in Fig.4.

The result show that L-J potential function and Morse function agree well with the curves in the long

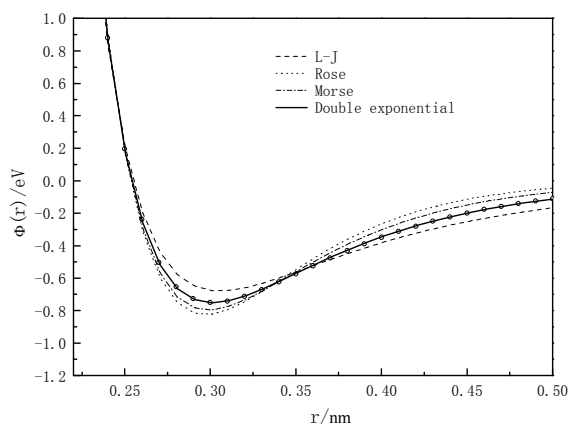


Fig.4 The comparison of the fitting results of these four potential functions

图 4 四种形式的势函数拟合数据结果的比较

range and short range of the potential function curve. The fitting effect of magnified observation curve shows that their global fitting effect is poor, and the accuracy is not high, although the correlation coefficients of the L-J potential function and the Morse potential function are higher, it meets the requirements. This will greatly affect the accuracy of calculation in the future calculation. The new double-exponential potential function performs very well in the overall fitting. The value of correlation coefficient is 1, indicating that the fitting quality is excellent. It is certain to provide strong precision support for the following calculation.

2 Application and Analysis

2.1 The calculation of phonon spectra of Platinum

To verify the reliability of the inversion potential, the phonon spectra of Platinum is calculated through using the module of GULP in the Material Studio. The calculation adopt inversion potential method, Sutton-Chen's many-body potential of EAM potential theory and the CASTEP module (using finite displacement method) in the software respectively, as shown in Fig.5.

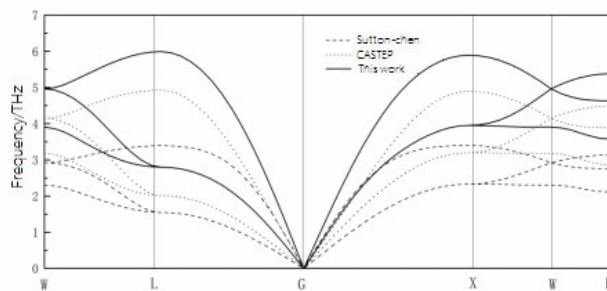


Fig.5 The phonon spectra of Pt

图 5 铂的声子谱图

The coordinate of these main symmetric points in the Brillouin Zone are G (0, 0, 0), X (0.5, 0, 0.5), W (0.5, 0.25, 0.75), K (0.75, 0.375, 0.375), L (0.5, 0.5, 0.5). The tendency of these curves is consistent, meant inversion potential can reflect the interaction between atoms efficiently. The EAM potential method needs 51 times more time in the computation comparing with

inversion potential method, indicating that the inversion method has great advantage in the amount of calculation. As for EAM potential function, it has a wide choice of function forms and more empirical factors^[18]. Its equation is deduced based on the Rose potential function, which leads to the unreliable calculation results. Yet inversion potential based on the number theory, through strict mathematical proof, is an overall accuracy potential. The calculation of phonon spectra is effective and reliable.

2.2 The verification and calculation of the potential function

Eq.(8) is used to fit the lattice cohesive energy curve as shown in Fig. 2. Fitting parameters are shown in Table 4. The value of correlation coefficient is 0.99996.

$$u(r) = D_1 \exp[-\alpha(r - R_0)] - D_2 \exp[-\beta(r - R_0)] \quad (8)$$

The first derivative equals to zero of the lattice cohesive energy with respect to the relative distance r , which leads to the nearest atom distance in equilibrium state of 0 K. The value of the nearest atom distance of Pt is $r_0^{\text{Pt}} = 0.27702$ nm. The lattice structure of Pt is optimized by using the inversion potential function (GULP module), and the value of the nearest atom distance is $r_0^{\text{Pt}} = 0.27702$ nm. Compared with the lattice constants $r_0^{\text{Pt}} = 0.27702$ nm in the experiment^[17], the cohesive energy function and the inversion potential function are both accurate and effective. Physical quantities such as linear expansion coefficient, bulk modulus, and Grüneisen constant are calculated. Then the calculation results are compared with experimental data.

Tab.4 Fitting parameters of cohesive curve using double exponential potential function

表 4 用双指数函数拟合得到的晶格内聚能曲线参数

| Element | D_1/eV | $\alpha/(1/\text{nm})$ | D_2/eV | $\beta/(1/\text{nm})$ | R_0/nm |
|---------|-----------------|------------------------|-----------------|-----------------------|-----------------|
| Pt | 2.13453 | 0.376381 | 9.34367 | 0.123552 | 0.291362 |

2.2.1 The calculation of linear expansion coefficient

The calculation method is based on the calculated formula of the potential function and the Boltzmann statistics equation^[16], which can calculate the atomic average thermal vibration displacements at different

temperature, and can be written as:

$$\bar{\delta} = \int_{-\infty}^{\infty} \delta e^{-V/k_B T} d\delta / \int_{-\infty}^{\infty} e^{-V/k_B T} d\delta \quad (9)$$

where $\delta = r - r_0$, r_0 represents the nearest atom distance in equilibrium state of 0 K. Considering each atom has a certain size, r_0 must be a value varies from a to ∞ , where a represents the ionic radius of Pt, resulting in:

$$\bar{\delta} = \int_a^{\infty} r e^{-V(r)/k_B T} dr / \int_a^{\infty} e^{-V(r)/k_B T} dr - r_0 \quad (10)$$

The linear expansion coefficient is a one-dimensional quantity, and $V(r)$ is the One-dimensional quantity of lattice cohesive energy, while $u(r)$ is the three-dimensional quantity of lattice cohesive energy. So the relationship between $V(r)$ and $u(r)$ is

$$V(r) = u(r)/3 \quad (11)$$

Bring Eq.(8) and the data in Table 4 into Eq.(10), the value of volume change under the temperature range from 273K to T_M are calculated using self-compiled programs. The values of the coefficient of expansion under different temperatures are obtained, and the α - T curve is obtained, as shown in Fig.6. Compared with the experimental data^[20], it's found that the trends of the curves are almost identical. The linear expansion coefficient (293K) is calculated as $\alpha_L^{\text{Pt}} = 7.07 \times 10^{-6} \text{K}^{-1}$. Comparing with the experimental data^[20] $\alpha_L^{\text{Pt}} = 8.8 \times 10^{-6} \text{K}^{-1}$, the relative error is 19.6%.

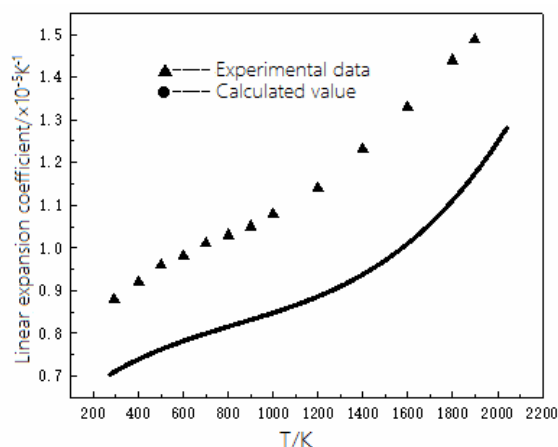


Fig.6 The linear expansion coefficient curves of Pt

图 6 铂的热膨胀系数的实验和计算值

2.2.2 The calculation of bulk modulus

According to the calculation results in 2.2.1 section, the bulk modulus of elasticity at different temperatures can be calculated by the cohesive energy

function in theory. Considering the calculation results at room temperature is more reference value, the cohesive energy function to calculate the elastic modulus at room temperature, and compared with the calculated results of inversion potential (using GULP module) and experimental data, as shown in Tab.5.

Tab.5 The bulk moduli calculation of Pt

表 5 计算得到的铂的体模量

| The bulk moduli/GPa | The cohesive energy function (293K) | The inversion potential(0K) | experimental data (293K) |
|---------------------|-------------------------------------|-----------------------------|--------------------------|
| κ_{Pt} | 308.60 | 316.31 | 276 |

Compare with experimental data, the relative error is 11.8%, meant the calculation method is accurate and effective.

2.2.3 The calculation of Grüneisen constant

According to Grüneisen equation,

$$\gamma = \kappa \alpha_V V / C_V \quad (12)$$

where κ represents bulk modulus, α_V represents volumetric expansion coefficient, the relationship between α_V and α_L is $\alpha_V = 3\alpha_L$, γ represents Grüneisen constant, C_V represents the specific heat at constant volume.

The value of κ and α_V calculated above, and equation $V = N_A (\sqrt{2}r_0)^3 / 4$, where N_A represents the Avogadro's number and r_0 represents nearest atomic distance in Equilibrium state, the value of Grüneisen constant γ at 293K is achieved as $\gamma_{Pt} = 2.64$. Whereas the experimental data^[20] $\gamma_{Pt} = 3.03$, the relative error is 12%, meant the result is accurate and effective^[23-25].

3 Conclusion

1) The inversion pair potential curve of Platinum is generated.

2) The accurate pair potential function is obtained through fitting by the new double-exponential function.

3) The phonon spectra are calculated through using the inversion potential data, the EAM (embedded atom method) potential theory and first principle method respectively to verify the reliability

of the inversion potential.

4) The method combining Boltzmann statistics equation with lattice cohesive energy curve is proposed to calculate the thermal expansion coefficient.

5) The bulk modulus and Grüneisen constant in the room temperature are calculated.

The results are in good agreement with experiment results, which implies that the inversion potential is effective and accurate.

References:

- [1] LONG Y, CHEN N X. Theoretical study of (Ag, Au and Cu)/Al₂O₃ interfaces[J]. Journal of physics-condensed matter, 2009, 21(31): 315003.
- [2] SONG H Q, SHEN J, QIAN P, et al. Interfacial for Ag/GaN(0001) interfaces by inversion of adhesive energy[J]. Physica B, 2013, 431: 97-101.
- [3] ZHANG C H, HUANG S, LI R Z, et al. Effects on mechanical properties of refractory metal doped Ti₃Al alloy [J]. International journal of modern physics B, 2013, 27: 1350147.
- [4] ZHANG C H, HUANG S, SHEN J, et al. Chen' s lattice inversion embedded-atom method for Ni-Al alloy[J]. Chin phys B, 2012, 21(11): 113401.
- [5] LIU S J, SHI S Q, HUANG H, et al. Interatomic potentials and atomistic calculations of some metal hydride systems[J]. Journal of alloys and compounds, 2002, 330/332: 64-69.
- [6] WANG S M. The interaction potential between atoms in solid materials and the electron theory of elasticity in alkalis metals and alkaline-earth metals[J]. Scientia sinica (Series A), 1987(2): 170-178.
- [7] CHEN S, LU J S, XIE M, et al. First-principle investigation on mechanical performances of platinum-rhodium alloys[J]. Chinese journal of rare metals, 2015, 39(3): 276-282.
- [8] REN X L, CHEN S, XIE M, et al. Application and foundation on inversion lattice potential o gold and silver[J]. Acta Physica Sinica, 2015, 64(14): 147101.
- [9] REN X L, CHEN S, XIE M, et al. Research and foundation of inversion lattice potential of Pd[J]. Precious metals, 2017, 38(S1): 28-34.

- [10] REN X L, CHEN S, XIE M, et al. The foundation and study of a new type of lattice inversion potential for iridium[J]. International journal of modern physics B, 2015, 29(30): 1550220.
- [11] WANG Y D, CHEN N X. Atomistic study of misfit dislocation in metal/SiC(111) interfaces[J]. J phys: condens matter, 2010, 22: 135009-135018.
- [12] CHEN N X. Möbius inversion in physics[M]. Singapore: world scientific publishing Co. Pte. Ltd, 2012; 155-260.
- [13] XIA L, CHEN S, LU J S. The development and application of the interatomic potential of precious metals for molecular dynamics simulation[J]. Precious metals, 2013, 34(4): 82-87.
- [14] ZHANG J M, WU X J, HUANG Y H, et al. Energy calculation of the stacking fault in FCC metals by embedded-atom method[J]. Chin phys soc, 2006, 55(1): 393-397.
- [15] XIA L. The foundation and application of inversion potentials for the PtRh alloys[D]. Kunming: Kunming University of Science and Technology, 2013.
- [16] XIE Q, HUANG M C. Description of crystallographic direction families for perfect crystal and lattice sums[J]. Journal of Xiamen University (Natural Science), 1995, 34(1): 36-42
- [17] FLAHIVE P G, GRAHAM W R. Pair potential calculations of single atom self-diffusion activation energies[J]. Surface science, 1980, 91(2): 449-462.
- [18] ZHANG C H, HUANG S, LI R Z, et al. Structural and mechanical properties of Fe-Al compounds: An atomistic study by EAM simulation[J]. Intermetallics, 2014, 52: 68-91.
- [19] HU A, ZHANG W Y. Solid-state physics[M]. Beijing: Higher Education Press; 2008. Chapter 120, 3.
- [20] BRANDES E A, BROOK G B. Smithells metals reference book (7th ed)[M]. Oxford: Reed Educational and Publishing Ltd; 1992.
- [21] ZHANG B. Assessment and calculation of thermal expansion coefficient for metallic elements[D]. Xiangtan: Xiangtan University, 2014.
- [22] LIU C, ZHOU T, ZHENG R L. The expansion coefficient and elastic modulus of crystal with FCC structure[J]. Journal of Southwest China Normal University (natural science), 2006, 31(5): 83-87.
- [23] CHEN S, LIU Z G, CHEN D Q, et al. Summary of Au/Sn interdiffusion features[J]. 2005, 29(4): 413-417.
- [24] CHEN S, GENG Y H, WANG C J. Research progress of CoCrPt system targets fabrication[J]. Precious metals, 2013, 34(1): 74-78.
- [25] HU J Q, PAN Y, XIE M. First-principles study of phase stability and electronic properties of RhZr[J]. Transactions of Nonferrous Metals Society of China, 2011, 21: 2301-2305.